Using fluorescent probes and FRAP to investigate macromolecule diffusion in steam-exploded wood

Wood Science and Technology (2018) 52:1395–1410
https://doi.org/10.1007/s00226-018-1039-5

ORIGINAL

Using fluorescent probes and FRAP to investigate macromolecule diffusion in steam-exploded wood

Patric Kvist[1,3,4] · Erich Schuster[2,4] · Niklas Lorén[1,2,4] · Anders Rasmuson[1,3]

Received: 20 February 2018 / Published online: 25 July 2018

Abstract

Diffusion of fluorescently labeled dextran of varying molecular weight in wood pretreated by steam explosion was studied with a confocal microscope. The steam explosion experiments were conducted at relatively mild conditions relevant for materials biorefinery at a pressure of 14 bars for 10 min. The method of fluorescence recovery after photobleaching (FRAP) was used to perform diffusion measurements locally in the wood microstructure. It was found that the FRAP methodology can be used to observe differences in the diffusion coefficient based on localization in the microstructure, i.e., earlywood, latewood, and cell wall. Microscopic changes due to steam explosion were seen to increase diffusion of the smaller 3-kDa dextran diffusion probe in the earlywood, while the latewood structure was not affected in any significant way. Macroscopic changes to the structure in the form of ruptures due to the steam explosion pretreatment were observed to increase the rate of diffusion for the larger 40-kDa dextran probe.

Introduction

Biomass as a renewable resource is an important step toward a sustainable society by lowering the use of fossil fuels. The most abundant biomass resource is by far woody biomass (Liu et al. 2012), and integration of pulp mills into biorefineries, with the infrastructure already in place, is the key for the biorefinery concept (Gomes et al. 2014). The main goal of the material biorefinery is to produce value-added

✉ Anders Rasmuson
rasmuson@chalmers.se

[1] Department of Chemistry and Chemical Engineering, Chalmers University of Technology, 412 96 Gothenburg, Sweden

[2] Product Design and Perception, RISE Agrifood and Bioscience, Box 5401, 402 29 Gothenburg, Sweden

[3] Wallenberg Wood Science Center, The Royal Institute of Technology, Chalmers University of Technology, 100 44 Stockholm, Sweden

[4] SuMo Biomaterials, Chalmers University of Technology, Gothenburg, Sweden

products and materials from high molecular weight of cellulose, hemicellulose, and lignin. Other than the inherent polymers found in wood, enzymes are of interest in the biorefinery concept to aid in the hydrolysis of polysaccharides (Hasunuma et al. 2013). Diffusion of polysaccharides and enzymes are hindered by the wood microstructure (Wu et al. 2009; Kvist et al. 2017), and to increase the overall mass transport rate, a pretreatment step is often used.

Steam explosion (SE) is an extensively used physicochemical pretreatment method for biomass (Alvira et al. 2010) which can also be used at milder conditions to open up the structure for easier processability (Agbor et al. 2011). At harsher conditions, i.e., higher pressures, degradation of the main constituents takes place to a higher degree (Wang et al. 2009) and is desired if for example a bio-fuel platform is used. However, for the biorefinery focusing on materials, it is desired to retain large molecular weight of the constituents, thus milder conditions are favorable.

In SE, wood chips are treated with pressurized steam for a specific time period, and then the pressure is rapidly released, causing a pressure difference between the interior of the wood chips and the surrounding vessel, and finally the softened chips collide with other chips and the vessel walls (Muzamal et al. 2015). Chemical modifications occur during the steam treatment due to the high temperature of the steam, which can be observed by the dark discoloration of the wood (Zhang and Cai 2006). The rapid release of pressure has shown to increase the average pore diameter, attributed to removal of hemicellulose and lignin in combination with deformation of the cell wall (Muzamal et al. 2015). Further, the collisions of the soft wood chips after the pressure release cause significant physical damage, splits, and brush-like tears of the chips depending on the angle of impact (Muzamal et al. 2015; Muzamal and Rasmuson 2017).

Previous experiments on diffusion in wood have mostly utilized diffusion cells, measuring through diffusion of various ions (e.g., Cady and Williams 1935; Burr and Stamm 1947; Behr et al. 1952; Narayanamurti and Kumar 1953). More recent studies attempt to study the time-dependent ion concentration profiles by cutting the wood samples at different times prior to analysis (Kazi et al. 1996; Jacobson et al. 2006; Kolavali and Theliander 2013). Fluorescence recovery after photobleaching (FRAP) offers a nondestructive way of measuring diffusion as well as performing localized measurements inside a sample.

FRAP has emerged during the last two decades as a common and powerful method for measuring mass transport properties (Lorén et al. 2015). A confocal microscope is used to direct high-intensity light into a region of interest that will cause substantial photobleaching of the fluorescent molecules present in the area. This will impose a concentration gradient of non-bleached molecules in the region of interest, where unbleached molecules will diffuse into. The recovery of intensity in this area is a function of how fast unbleached molecules diffuse into the area. The local diffusion rate can be estimated from the rate of intensity recovery. Dextran labeled with the fluorophore fluorescein isothiocyanate (FITC) is commonly used as a diffusion probe in FRAP experiments (Deschout et al. 2014).

FRAP was first developed as a technique to measure the transport of proteins and lipids in living cells (Axelrod et al. 1976) and has been further developed and generalized (Kang et al. 2009) to include diffusion during the photobleaching step. This

technique has since then been used to study various different proteins in a number of cell membranes and living cells (Lorén et al. 2015). Apart from the field of cell biology, FRAP has found an important foothold in pharmaceutical research due to the technique's noninvasiveness and high specificity, making it possible to measure diffusion in vivo in complex materials (Deschout et al. 2014). Hydrogels have been especially interesting for a time-controlled drug delivery system where the heterogeneous structure inside the gel controls the delivery. Several studies have been conducted with FRAP to characterize the diffusive process in different gel structures (Hagman et al. 2012; Videcoq et al. 2013; Schuster et al. 2014, 2016; Lopez-Sanchez et al. 2015; Peixoto et al. 2015). FRAP has also been successfully used in food science where the microstructure of food often is a multiphase mixture of, for example, gels, foams, and emulsions (Wassén et al. 2014) where mass transport mechanisms control part of the final properties of the food product.

Model systems for mimicking parts of a cell wall in the form of gels have been investigated using the FRAP technique to study the influence of the size of the diffusion probe as well as the influence of the porous gel mesh size (Paës and Chabbert 2012). The hydrodynamic radius of dextran probes was found to influence diffusion more than the size of the mesh. On the other hand, the protein diffusion probes showed indications of anomalous diffusion, which they attributed to the interaction with the gel. Similarly, studies of the size dependency of molecules have been conducted by Yang et al. (2013), in which dextrans were used as diffusion probes. The porous structure was made from milled filter paper to evaluate the influence of pore size distribution on diffusion of the probe. Further studies on gel structures have been conducted using the FRAP technique to assess the effect of substrate hydrolysis and substrate binding on the mobility of enzymes (Cuyvers et al. 2011). Similar studies investigating binding and surface diffusion of cellulases on cellulose fibers have been performed using FRAP (Moran-Mirabal 2013). A more rigorous study on the mechanisms of carbohydrate-binding domains (CBMs) was carried out by Paës et al. (2015) utilizing FRAP and a set of similar CMBs in a variation of bioinspired assemblies. FRAP has recently been used to investigate diffusion in the wood cell wall for several types of chemical pretreatment methods for large-size dextran molecules (Paës et al. 2017).

The aim of the present study was to assess diffusion coefficients locally of large molecules in softwood pretreated with mild steam explosion used in the materials biorefinery concept. Fluorescently marked dextran of different size was used with the FRAP methodology on samples prepared with and without steam explosion. The inherent flexibility of FRAP with a confocal microscope is very suitable for the variations present in the wood microstructure as well as the local effects of the steam explosion pretreatment. Evaluation of the size of the diffusion probe as well as location within the wood structure was performed.

Materials and methods

Samples were prepared from a stem of Norway spruce (*Picea abies*) obtained from Södra (Värö, Sweden). The heartwood was cut into $4 \times 20 \times 130$ mm^3 rectangles and stored in airtight polyethylene bags in a freezer at -18 °C. FITC-dextran

of molecular weight 3, 10, and 40 kDa was purchased from Invitrogen Molecular Probes (Eugene, OR, USA).

Three different wood samples were prepared in order to analyze both physical and chemical effects of steam explosion: Untreated native wood as reference, steam-exploded wood (SEW), and steam-exploded and impacted wood (SEIW). The SEW samples are characterized by the discoloration due to high temperature steam and hydrolysis occurring. The pressure release causes an increase in porosity (Muzamal et al. 2015). The significance of the impact step for the SEIW samples, where the soft wood chips collide with other chips and vessel walls, is shown by distinct cracks and a further increase in porosity. Chemical analysis of samples for both residence time (Jedvert et al. 2012a) and temperature (Jedvert et al. 2012b) have shown that mainly small amounts of glucomannans extract during the process for short residence time (< 10 min).

The wood samples were defrosted for at least 24 h prior to use. Samples were further cut into smaller $4 \times 20 \times 20$ mm^3 pieces before steam explosion was performed. A total of 16 samples were used in the steam explosion equipment. The equipment is described elsewhere (Muzamal et al. 2015). Six of the samples were secured with a fixture to separate them from the impact step, while the rest were loaded as normal in the steam tank. The steam-exploded wood was obtained after introducing saturated steam at 14 bar (198 °C) in the steam tank for a total of 10 min. The pressure was quickly released to atmospheric conditions and the non-fixated samples rapidly escaped into the flash tank and collected along with the condensed steam. The steam-exploded and native samples are shown in Fig. 1. Depending on the collisions of wood chips in the flash tank, several different types of structural changes to the wood can occur which has been studied both experimentally and by mathematical modeling (Muzamal et al. 2015; Muzamal and Rasmuson 2017).

The dextran probes were diluted in deionized water. The probe concentration was 150 ppm, chosen to give a linear response in fluorescence versus concentration. A total of 20 ml of solution was prepared in polypropylene (PP) containers for each probe. The wood samples, as seen in Fig. 1, were impregnated with the probe solution using a vacuum-pressure cycle in an autoclave at room temperature (22 °C) based on Kolavali

Fig. 1 From left to right: native, SEW, and SEIW. Notice the color change after treatment present for both samples subjected to the steam explosion treatment. Furthermore the SEIW samples show distinct ruptures mostly along the fiber direction (color figure online)

and Theliander (2013). Vacuum was applied for 30 min after which the autoclave was pressurized with nitrogen at 5 bar for 1 h. The procedure was repeated for up to five cycles and when no floating pieces were observed the samples were assumed to be fully impregnated. The containers were sealed with tin foil to protect them from light source degradation and were stored in a refrigerator prior to use.

Fluorescence recovery after photobleaching (FRAP) measurements and imaging of the wood microstructure were carried out on a Leica SP5 confocal laser scanning microscope (CLSM) AOBS (Heidelberg, Germany). The light source used was an argon laser with an emission wavelength of 488 nm. A water immersion objective with a magnification of 20 and a numerical aperture (NA) of 0.50 was used throughout the study. Beam expander 1 was used, which lowered the effective NA to approximately 0.35 and yielded a slightly more cylindrical bleaching profile which will induce significant photobleaching above and below the focal plane thus avoiding diffusion along the optical axis (Deschout et al. 2010). It is crucial for the precision of the diffusion rate estimate that the depth of the cylindrical bleaching profile is considerably larger than the diameter of the bleaching region. If this condition is true, then the diffusion rate mainly depends on the radial diffusion, and a 2D model can be used, which substantially simplifies the calculations (Lorén et al. 2015).

The saturated wood samples were prepared for the microscope by slicing 200–300-µm-thick sections perpendicular to the fiber direction with a high-profile disposable blade. The cut section was subsequently mounted on a cover glass in a well created with three layers of Secure Seal™ adhesive spacers (ThermoFischer Scientific, Sweden), according to Fig. 2. About 10 µl of additional probe solution was added to keep the sample completely covered in solution after which a second cover glass was used to seal the created well.

The FRAP measurements were carried out at room temperature (22 °C) with the following settings: image format 256×256 pixels, zoom factor 4 (with a zoom-in during bleaching), and scanning rate 1000 Hz, rendering an image acquisition rate of 0.265 s per image and a pixel size of 0.73 µm. The FRAP images were stored as 12-bit tiff images. The images were recorded using a PMT detector.

The FRAP protocol consisted of 20 pre-bleach images, 1–4 bleach images depending on the probe followed by 50 images during the recovery process, depicted schematically in Fig. 3. Five measurements were performed per region investigated. Here, bleaching refers to the stage where a higher laser intensity is applied to photobleach some of the fluorescent molecules in the region of interest, seen as the drop from (a) to (b) in Fig. 3.

In a heterogeneous sample, it is common that the efficiency of the bleaching is varying depending on the local sample transparency. In addition, different diffusion probes need slightly different amounts of laser power to obtain similar degree of bleaching.

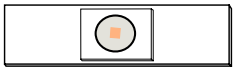

Fig. 2 Cut cross-sectional wood sample mounted on a cover glass with a secure seal creating a circular well. Solution of dextran probes is added to the well in excess to completely surround the wood sample

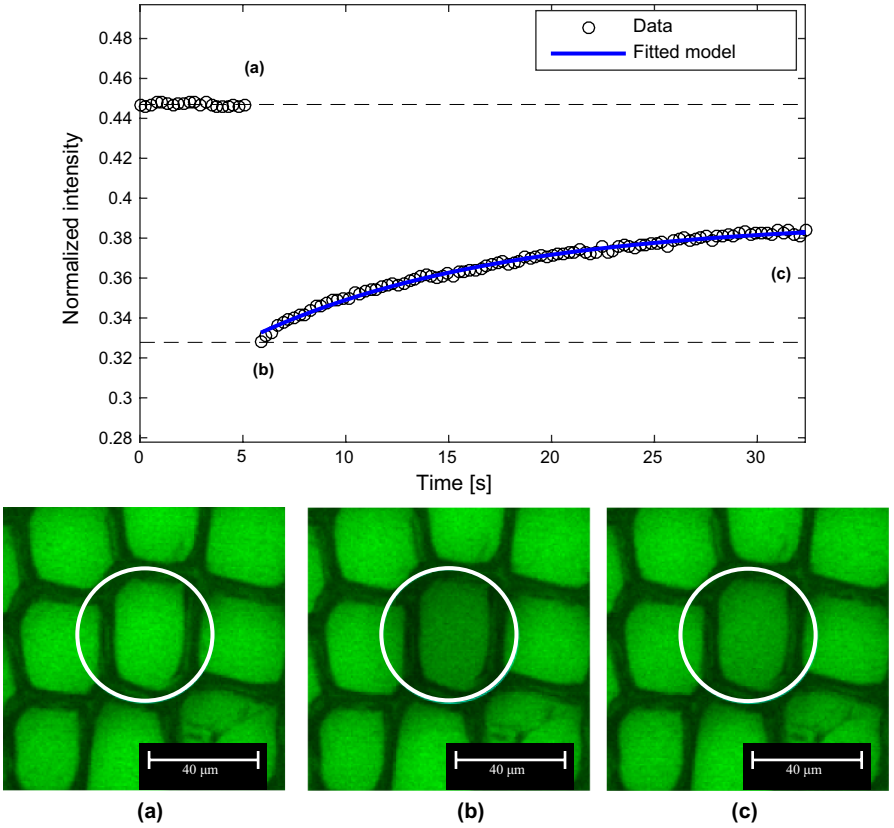

Fig. 3 A typical FRAP measurement with the 50 µm circular ROI for a lumen, including micrographs at three different time points as indicated in the recovery curve above **a** Pre-bleach, **b** bleach, **c** post-bleach. Figure **a** is from the pre-bleached period and is indicated on the intensity curve before the drop in intensity, **b** is after the photobleaching and the subsequent drop in intensity, and **c** is at the end of the post-bleaching period

Thus, to perform consistent measurements, the number of bleaching images was adjusted to achieve an initial bleaching degree of approximately 30% of the pre-bleach intensity. The laser intensity was adjusted using AOTF (acusto-optical tunable filters) to be low during pre- and post-bleach to avoid unwanted bleaching effects while during bleaching the intensity was high.

Two different pixel-based frameworks were used to process the data from the FRAP measurements. The bulk of the measurements were performed with a circular region of interest (ROI) utilizing a model (Jonasson et al. 2008) assuming an initial photobleaching profile that is approximately Gaussian. The circular ROI fits well with the tracheid cells in wood. For more specific cell wall measurements, the more flexible method of rectangular FRAP (rFRAP) (Deschout et al. 2010) was used. An important assumption in the rFRAP is a linear photobleaching process which means that only a small amount of bleaching is allowed. It

was shown in a validation experiment with FITC-dextran in sucrose solution that rFRAP is independent of the amount of photobleaching up to 50% (Deschout et al. 2010). All FRAP data evaluations were performed in MATLAB (MathWorks, USA).

The region of interest (ROI) was chosen such that consistent measurements could be performed on the different samples. To investigate the lumen to lumen diffusion rates, circular ROIs were used to completely bleach the entire lumen, including the cell wall, to achieve consistent bleaching along the fiber direction. The circular ROIs were placed adjacent to both ray parenchyma cells and the interface between earlywood and latewood to investigate the effect of structural elements on diffusion rates, compared to lumens only surrounded by other lumens.

Figure 4 shows a CLSM micrograph seen from the view of the microscope in which the cell wall auto-fluorescence is visible. The signal is clearly the strongest in the middle lamella where the lignin content is the highest. Other features that can be seen are the bordered pit pair as well as a ray parenchyma cell perpendicular to the direction of the lumen. A clear interface between the larger earlywood lumen and the smaller latewood lumen differentiates the figure in the middle.

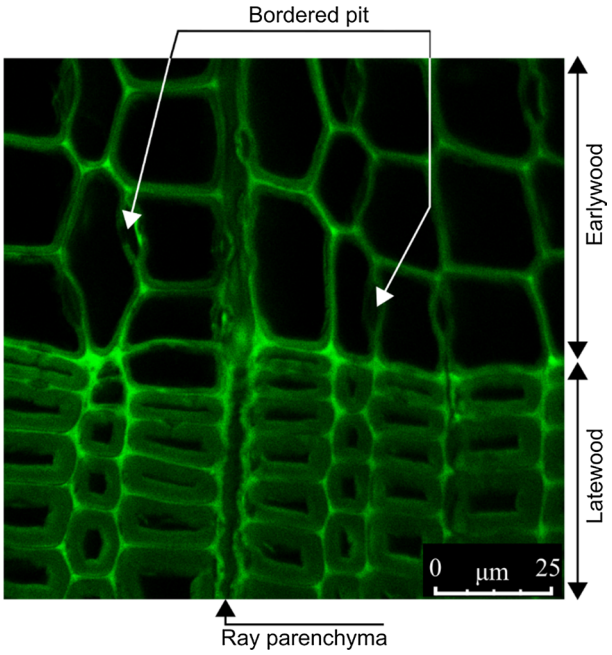

Fig. 4 CLSM micrograph of water-impregnated cross-sectional slice of non-treated spruce for an excitation wavelength of 488 nm. The autofluorescent signal in the emission range of 500–650 nm from lignin is seen to emerge from the cell wall, with the strongest signal from the middle lamella

Results and discussion

Diffusion coefficients ($\mu m^2/s$) obtained from the FRAP measurements are presented in four sections. The first section presents the free diffusion coefficient of the dextran probes in solution. This is followed by radial diffusion between lumens to investigate the effect of the steam explosion pretreatment as well as the size of the probe. Diffusion in the latewood cell wall is presented in the third section. The fourth section deals with physical structural modifications of the microstructure and its effect on diffusion locally.

Measurements were performed with at least five replications for each sample and each diffusion probe for the majority of the experiments. For the impacted wood samples in the last section, two replications at each enumerated position were performed. Some of the samples show signs of compression which might have influenced the FRAP measurements. However, nothing is known of the relative diffusion in compression wood which is more highly lignified relative to that of normal wood so this is of unknown significance. To assess the statistical significance of the diffusion probes, an ANOVA two-way analysis with a subsequent multiple comparison test by the Tukey–Kramer method for the significant main effects was performed within a 95% confidence interval for the true mean difference performed in MATLAB (MathWorks, USA).

Free diffusion of dextran

FRAP measurements were performed on the dextran dissolved in aqueous solution to obtain the free diffusion coefficient, i.e., the coefficient without any obstructions present. Low molecular weight dextran diffuses relatively fast compared to the higher molecular weight as seen by the higher diffusion coefficients in Table 1. For an estimate of the size of each probe, the hydrodynamic radius was calculated based on the Stokes–Einstein equation (Cussler 2009). The solutions were assumed to be dilute enough to ensure little to no interaction between the molecules. The results obtained for the free diffusion coefficient for ROI sizes larger than 10 μm coincide well with previous studies (Arrio-Dupont et al. 1996) as shown in Fig. 5.

For smaller ROI sizes (< 10 μm), the amount of pixels in the region reaches a critical point and the FRAP measurement becomes more difficult to analyze accurately.

Table 1 Free diffusion coefficients D_0 in $\mu m^2/s$ of dextran in aqueous solutions. The hydrodynamic radius in nm was estimated by the Stokes–Einstein equation (Cussler 2009) based on the diffusion coefficient obtained from the FRAP measurements

Diffusion probe	Molecular weight (kDa)	Diffusion coefficient ($\mu m^2/s$)	Hydrodynamic radius (nm)
FITC-dextran	3	154.3 ± 1.9	1.59 ± 0.02
	10	75.6 ± 1.3	3.25 ± 0.05
	40	42.6 ± 0.6	5.76 ± 0.08

It was found that the 40-kDa dextran had least variations among the probes for ROI sizes down to 3 µm. As such, this probe was used exclusively for measurements when small ROI sizes were required.

Radial diffusion from lumen to lumen: Effect of explosion, impact, and size of probe

To investigate the effect of local microscopic elements on radial diffusion in the earlywood structure, three different locations were used; see Fig. 6. Structures include lumens adjacent to ray cells and the interface between early- and latewood compared to a lumen only adjacent to other lumens. This also served as guidelines for consistent measurement between the wood samples due to the inherent variability present in the microscopic structure.

The result for the 3-kDa dextran diffusion probe is presented in Fig. 7, based on the three ROI setups stated above for the three wood samples. The native sample is shown to have the lowest diffusion coefficient while a subsequent increase is seen for the SEW and SEIW samples. However, no significant difference was observed for measurements adjacent to ray parenchyma cells nor the interface between early- and latewood.

Contrary to what was observed for the 3-kDa probe, no significant difference can be seen for the two larger probes among the wood samples, presented in Fig. 8. All three probes indicate no significant difference in radial diffusion due to adjacent microscopic structural elements.

SEIW samples have a large variety in structural modifications and for the results here samples were chosen such that they could directly be compared with the native and SEW samples. Thus, parts of the SEIW sample without ruptures were chosen,

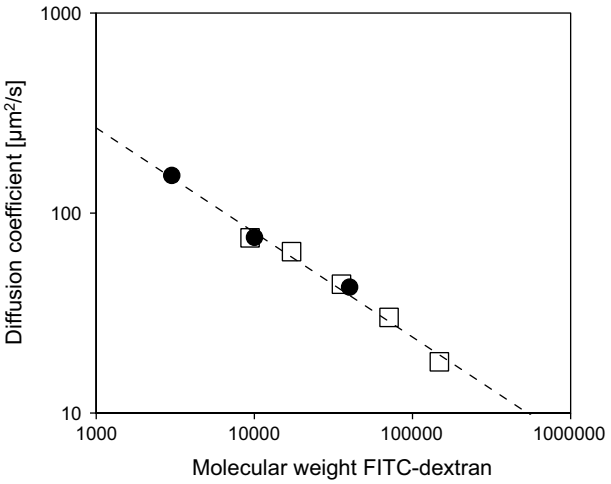

Fig. 5 Molecular weight dependence reproduced from Arrio-Dupont et al. (1996) of FITC-dextrans in aqueous solution indicated by squares with the corresponding fitted dashed line. Black circles were measured in this study

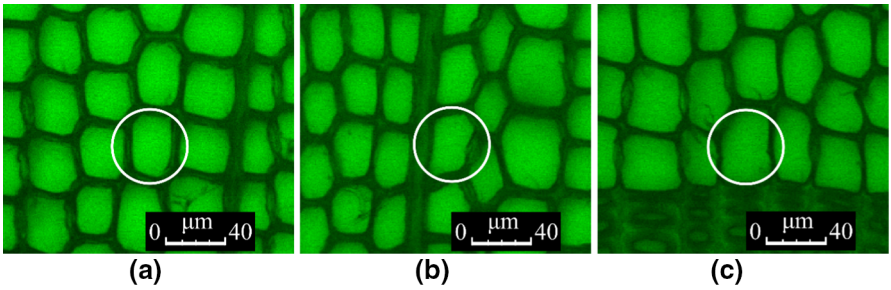

Fig. 6 Experimental ROI setup for earlywood diffusion measurements. ROI size was 50 µm **a** Lumen, **b** ray cell, **c** interface. In **b** and **c** the ROI is placed over a lumen adjacent to a ray channel and the interface between early- and latewood, respectively, compared to **a** where the lumen is only adjacent to other lumens

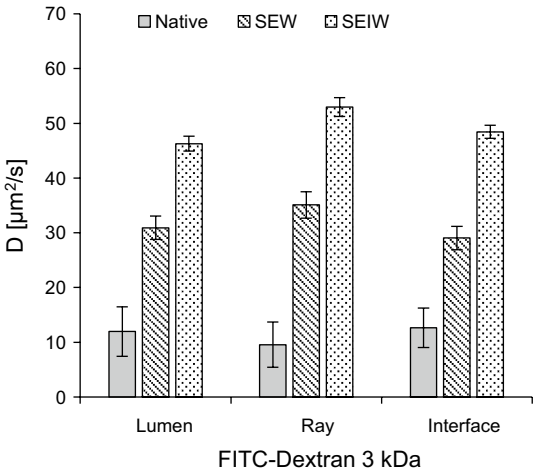

Fig. 7 Diffusion coefficients in $\mu m^2/s$ for FITC-dextran of 3 kDa. The FRAP measurements were performed adjacent to ray parenchyma cells, the interface between early- and latewood, and lumens. FRAP measurements were performed according to the ROI setup described in Fig. 6 for all wood samples

and the main observable difference of the earlywood was that the cell wall was less rigid. The result shows that the diffusion coefficient is dependent on treatment for the smallest probe but not for the larger probes. This could be due to small increases in cell wall porosity due to removal of lignin and hemicelluloses (Donaldson et al. 1988) as well as microcracks caused by the impact after the rapid pressure release (Muzamal et al. 2015).

For latewood, consistent distinct features are much more variable and harder to ascertain compared to earlywood. Instead, a fixed circular ROI size of 25 µm was used and lumens of consistent size were focused on, as shown in Fig. 9a.

Results are presented in Fig. 9b. Some variations among the samples can be seen which is most likely due to the difficulty in performing consistent measurements between the samples. However, no significant difference for neither the diffusion probe size nor sample pretreatment is observed for latewood. Compared to earlywood, the diffusion coefficient in latewood is lower, especially for the 3 kDa

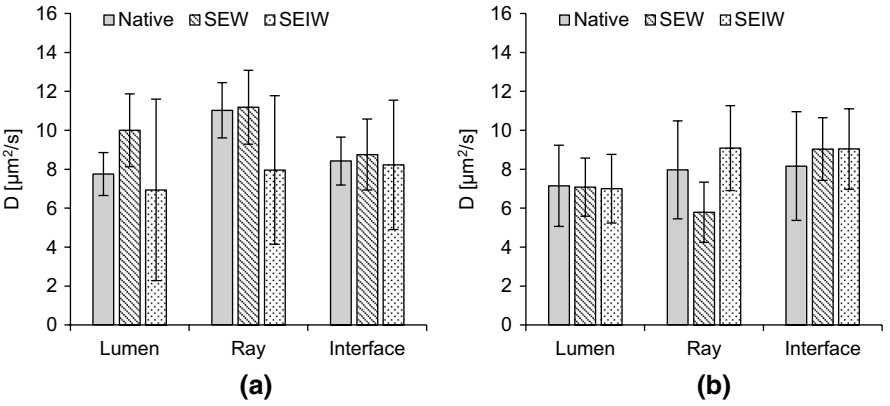

Fig. 8 Diffusion coefficients in µm²/s for FITC-dextran of 10 kDa and 40 kDa. The FRAP measurements were performed adjacent to ray parenchyma cells, the interface between early- and latewood, and lumens. FRAP measurements were performed according to the ROI setup described in Fig. 6 for all wood samples. **a** FITC-dextran 40 kDa, **b** FITC-dextran 10 kDa

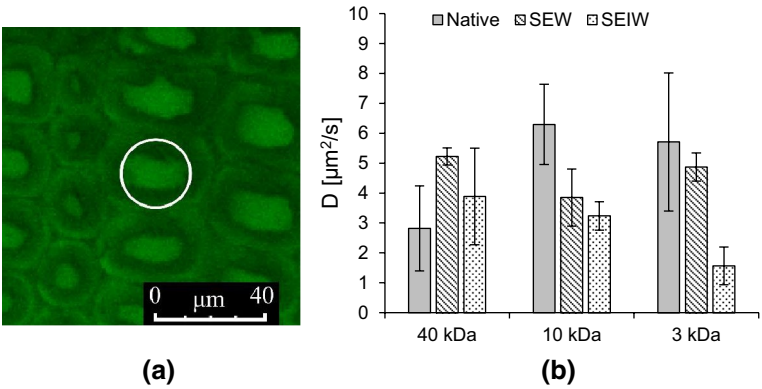

Fig. 9 Experimental ROI setup for latewood diffusion measurements in **a**. ROI size was 25 µm. In **b** corresponding diffusion coefficients in µm²/s for FITC-dextran of 3, 10, and 40 kDa. FRAP measurements were performed with the same setup for all wood samples

dextran. The treatment does not seem to affect the dense structure of the latewood to any degree for samples without cell wall ruptures.

Diffusion in the cell wall

Additional cell wall measurements were primarily taken of latewood due to the thicker cell walls present in that part of the wood structure, with a rectangle ROI size of 3 µm for the 40-kDa diffusion probe.

Figure 10 shows the results and ROI setup of cell wall measurements for both native and SEIW samples. As expected, the results show high obstruction due to the cell wall; however, no difference was found between the native and SEIW samples.

Localization in the cell wall is seen to have an influence on the diffusion coefficient. The corner lamella coefficient is larger by a factor 4 compared to the center of the cell wall.

Diffusion in impacted wood

More severe structural changes in the form of ruptures in the microstructure occur during the impact step in steam explosion. One such case is presented in Fig. 11a where a rupture has caused a separation between early- and latewood as well as damage to the cell walls. Measurements were performed around the separation for the largest dextran probe, enumerated in Fig. 11a.

In the large void caused by the separation, the diffusion coefficient has approached the free diffusion coefficient (1–4 in Fig. 11b) and the nearby cell walls have little to no effect, as should be expected. For nearby lumens close to the rupture (5–7 in Fig. 11b), the diffusion coefficient is lower indicating that the probe is somewhat obstructed.

In Fig. 12a, local effects on the earlywood structure are seen. The rupturing of cell walls forms a channel in the radial direction in the microstructure perpendicular to the fiber direction. In the open space of the channel (1–4 and 6 in Fig. 12b), the results are approaching the free diffusion coefficient (42 $\mu m^2/s$), however it is slightly lower than in the previously larger void in Fig. 11. For the nearby lumens (5 and 7 in Fig. 12b), the drop in diffusion coefficient shows the obstruction of the cell wall on the dextran probe.

Conclusion

The FRAP methodology was successfully used to obtain diffusion coefficients locally within the native and steam-exploded wood for dextran molecules of molecular weight similar to that which is relevant in a material driven biorefinery, such as

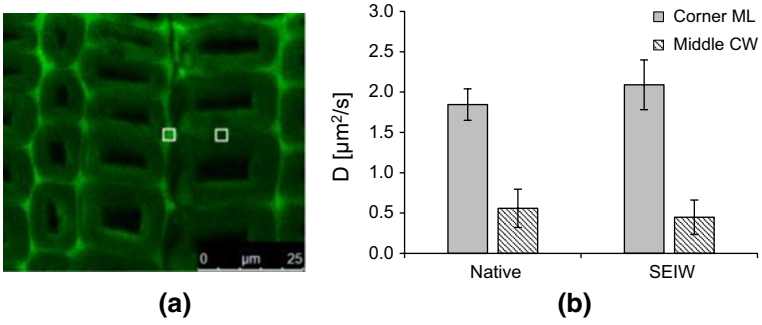

Fig. 10 Experimental ROI setup for cell wall diffusion measurements in **a**. A quadratic ROI size of 3 µm was used for a more flexible setup with focus on the corner of the middle lamella (ML) and in the middle of the cell wall (CW). In **b** corresponding diffusion coefficients in $\mu m^2/s$ for FITC-dextran of 40 kDa. FRAP measurements were performed with the same setup for native and SEIW samples

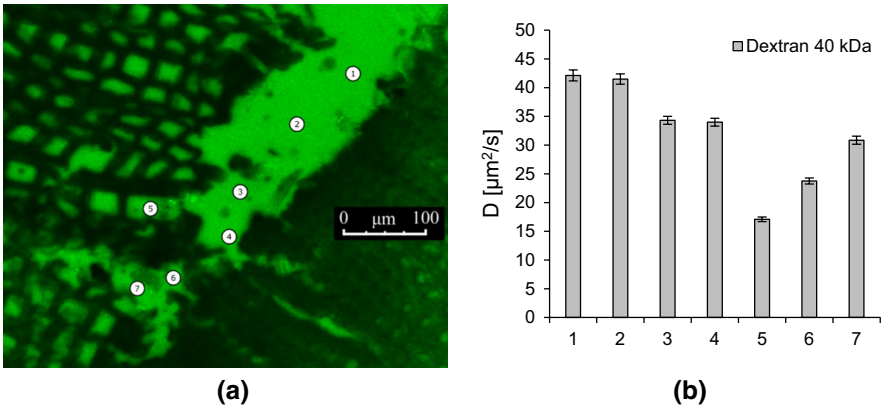

Fig. 11 CLSM micrograph **a** of SEIW sample. The rupture that has occurred between the dense latewood is seen to the right and earlywood to the left. FRAP measurements were performed at the enumerated circles (1–7) indicated on the micrograph. A circular ROI of 10 µm was used. In **b** corresponding diffusion coefficients in $\mu m^2/s$ for FITC-dextran of 40 kDa. FRAP measurements were performed only for SEIW samples

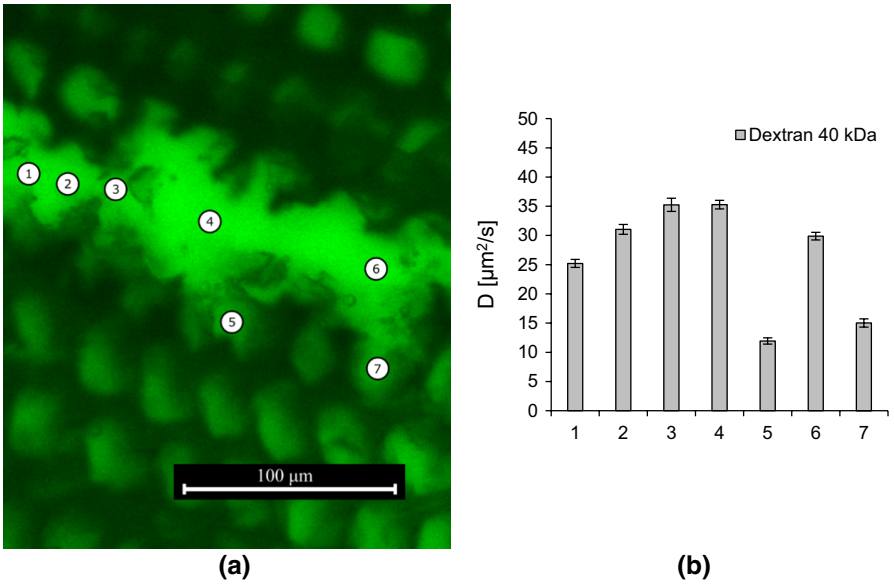

Fig. 12 CLSM micrograph **a** of a SEIW sample with ruptured cell walls forming a channel in earlywood. FRAP measurements were performed at the enumerated circles (1–7) indicated on the micrograph. A circular ROI of 10 µm was used. In **b** corresponding diffusion coefficients in $\mu m^2/s$ for FITC-dextran of 40 kDa. FRAP measurements were performed only for SEIW samples

enzymes and polysaccharides. Results show a range of diffusivities obtained in the different microscopic structures in wood from earlywood, latewood, cell wall, and structural deformation due to the steam explosion pretreatment. It was observed that the microscopic changes in the earlywood cell wall due to pretreatment gave rise to an increase in diffusion of the smaller dextran of 3 kDa. Macroscopic changes, such as ruptures and tears in the cell wall, were seen to increase the rate of diffusion for the larger 40-kDa dextran close to the damaged structure. Localization in the latewood cell wall was seen to affect the diffusion coefficient. The corner middle lamella had higher diffusion rates compared to the middle of the cell wall.

Previous studies have shown an increase in porosity by mild steam explosion attributed to removal of hemicellulose and lignin as well as the deformation of the internal structure of the cell wall due to the rapid pressure release. The flexibility of the FRAP methodology made it possible to locally investigate these changes and to better understand how it affects the overall diffusion rates.

Acknowledgements The authors would like to thank Wallenberg Wood Science Center for financial support and SuMo Biomaterials for support with confocal microscopy.

References

Agbor VB, Cicek N, Sparling R, Berlin A, Levin DB (2011) Biomass pretreatment: fundamentals toward application. Biotechnol Adv 29:675–685. https://doi.org/10.1016/j.biotechadv.2011.05.005

Alvira P, Tomás-Pejó E, Ballesteros M, Negro MJ (2010) Pretreatment technologies for an efficient bioethanol production process based on enzymatic hydrolysis: a review. Bioresour Technol 101:4851–4861. https://doi.org/10.1016/j.biortech.2009.11.093

Arrio-Dupont M, Cribier S, Foucault G, Devaux PF, D`Albis A (1996) Diffusion of fluorescently labeled macromolecules in cultured muscle cells. Biophys J 70:2327–2332. https://doi.org/10.1016/S0006-3495(96)79798-9

Axelrod D, Koppel DE, Schlessinger J, Elson E, Webb WW (1976) Mobility measurement by analysis of fluorescence photobleaching recovery kinetics. Biophys J 16:1055–1069. https://doi.org/10.1016/S0006-3495(76)85755-4

Behr EA, Briggs DR, Kaufert FH (1952) Diffusion of dissolved materials through wood. J Phys Chem 57:476–480

Burr HK, Stamm AJ (1947) Diffusion in wood. J Phys Chem 51(1):240–261

Cady LC, Williams JW (1935) Molecular diffusion into wood. J Phys Chem 39:87–102

Cussler EL (2009) Diffusion, mass transfer in fluid systems, 3rd edn. Cambridge University Press, Cambridge

Cuyvers S, Hendrix J, Dornez E, Engelborhs Y, Delcour JA, Courtin CM (2011) Both substrate hydrolysis and secondary substrate binding determine xylanase mobility as assessed by FRAP. J Biol Chem 115:4810–4817

Deschout H, Hagman J, Fransson S et al (2010) Straightforward FRAP for quantitative diffusion measurements with a laser scanning microscope. Opt Expr. https://doi.org/10.1364/OE.18.022886

Deschout H, Raemdonck K, Demeester J, De Smedt SC, Braeckmans K (2014) FRAP in pharmaceutical research: practical guidelines and applications in drug delivery. Pharm Res 31:255–270. https://doi.org/10.1007/s11095-013-1146-9

Donaldson LA, Wong KKY, Mackie KL (1988) Ultrastructure of steam-exploded wood. Wood Sci Technol 22:103–114. https://doi.org/10.1007/BF00355846

Gomes FJB, Santos FA, Colodette JL, Demuner IF, Batalha LAR (2014) Literature review on biorefinery processes integrated to the pulp industry. Nat Resour 5:419–432. https://doi.org/10.4236/nr.2014.59039

Hagman J, Lorén N, Hermansson AM (2012) Probe diffusion in κ-carrageenan gels determined by fluorescence recovery after photobleaching. Food Hydrocoll 29:106–115. https://doi.org/10.1016/j.foodhyd.2012.02.010

Hasunuma T, Okazaki F, Okai N, Hara KY, Ishii J, Kondo A (2013) A review of enzymes and microbes for lignocellulosic biorefinery and the possibility of their application to consolidated bioprocessing technology. Bioresour Technol 135:513–522. https://doi.org/10.1016/j.biortech.2012.10.047

Jacobson AJ, Smith GD, Yang R, Banerjee S (2006) Diffusion of sulfide into Southern pine (*Pinus taeda* L.) and sweetgum (*Liquidambar styraciflua* L.) particles and chips. Holzforschung 60:498–502. https://doi.org/10.1515/HF.2006.082

Jedvert K, Saltberg A, Lindström ME, Theliander H (2012a) Mild steam explosion and chemical pretreatment of Norway spruce. BioResources 7:2051–2074

Jedvert K, Wang Y, Saltberg A, Henriksson G, Lindström ME, Theliander H (2012b) Mild steam explosion: a way to activate wood for enzymatic treatment, chemical pulping and biorefinery processes. Nord Pulp Pap Res J 27:828–835. https://doi.org/10.3183/NPPRJ-2012-27-05-p828-835

Jonasson JK, Loren N, Olofsson P, Nyden M, Rudemo M (2008) A pixel-based likelihood framework for analysis of fluorescence recovery after photobleaching data. J Microsc 232:260–269. https://doi.org/10.1111/j.1365-2818.2008.02097.x

Kang M, Day CA, Drake K, Kenworthy AK, DiBenedetto E (2009) A generalization of theory for two-dimensional fluorescence recovery after photobleaching applicable to confocal laser scanning microscopes. Biophys J 97:1501–1511. https://doi.org/10.1016/j.bpj.2009.06.017

Kazi KMF, Gauvin H, Jollez P, Chornet E (1996) A diffusion model for the impregnation of lignocellulosic materials. Tappi 80:209–219

Kolavali R, Theliander H (2013) Determination of the diffusion of monovalent cations into wood under isothermal conditions based on LiCl impregnation of Norway spruce. Holzforschung 67:559–565. https://doi.org/10.1515/hf-2012-0182

Kvist P, Therning A, Gebäck T, Rasmuson A (2017) Lattice Boltzmann simulations of diffusion through native and steam-exploded softwood bordered pits. Wood Sci Technol 51(6):1261–1276. https://doi.org/10.1007/s00226-017-0938-1

Liu S, Lu H, Hu R, Shupe A, Lin L, Liang B (2012) A sustainable woody biomass biorefinery. Biotechnol Adv 30:785–810. https://doi.org/10.1016/j.biotechadv.2012.01.013

Lopez-Sanchez P, Schuster E, Wang D, Gidley MJ, Strom A (2015) Diffusion of macromolecules in self-assembled cellulose/hemicellulose hydrogels. Soft Matter 11:4002–4010. https://doi.org/10.1039/C5SM00103J

Lorén N, Hagman J, Jonasson JK, Deschout H (2015) Fluorescence recovery after photobleaching in material and life sciences: putting theory into practice. Q Rev Biophys 48:323–387. https://doi.org/10.1017/S0033583515000013

Moran-Mirabal JM (2013) The study of cell wall structure and cellulose-cellulase interactions through fluorescence microscopy. Cellulose 20:2291–2309. https://doi.org/10.1007/s10570-013-0010-8

Muzamal M, Rasmuson A (2017) Dynamic simulation of disintegration of wood chips caused by impact and collisions during the steam explosion pretreatment. Wood Sci Technol 51:115–131. https://doi.org/10.1007/s00226-016-0840-2

Muzamal M, Jedvert K, Theliander H, Rasmuson A (2015) Structural changes in spruce wood during different steps of steam explosion pretreatment. Holzforschung 69:61–66. https://doi.org/10.1515/hf-2013-0234

Narayanamurti D, Kumar VB (1953) Diffusion of organic molecules through wood. J Polym Sci 10:515–524. https://doi.org/10.1002/pol.1953.120100602

Paës G, Chabbert B (2012) Characterization of arabinoxylan/cellulose nanocrystals gels to investigate fluorescent probes mobility in bioinspired models of plant secondary cell wall. Biomacromolecules 13:206–214. https://doi.org/10.1021/bm201475a

Paës G, von Schantz L, Ohlin M (2015) Bioinspired assemblies of plant cell wall polymers unravel the affinity properties of carbohydrate-binding modules. Soft Matter 11:6586–6594. https://doi.org/10.1039/C5SM01157D

Paës G, Habrant A, Ossemond J, Chabbert B (2017) Exploring accessibility of pretreated poplar cell walls by measuring dynamics of fluorescent probes. Biotechnol Biofuels 10:15. https://doi.org/10.1186/s13068-017-0704-5

Peixoto PDS, Bouchoux A, Huet S et al (2015) Diffusion and partitioning of macromolecules in casein microgels: evidence for size-dependent attractive interactions in a dense protein system. Langmuir 31:1755–1765. https://doi.org/10.1021/la503657u

Schuster E, Eckardt J, Hermansson A-M et al (2014) Microstructural, mechanical and mass transport properties of isotropic and capillary alginate gels. Soft Matter 10:357–366. https://doi.org/10.1039/c3sm52285g

Schuster E, Sott K, Ström A et al (2016) Interplay between flow and diffusion in capillary alginate hydrogels. Soft Matter 12:3897–3907. https://doi.org/10.1039/c6sm00294c

Videcoq P, Steenkeste K, Bonnin E, Garnier C (2013) A multi-scale study of enzyme diffusion in macromolecular solutions and physical gels of pectin polysaccharides. Soft Matter 9:5110–5118. https://doi.org/10.1039/c3sm00058c

Wang K, Jiang JX, Xu F, Sun RC (2009) Influence of steaming explosion time on the physic-chemical properties of cellulose from Lespedeza stalks (*Lespedeza crytobotrya*). Bioresour Technol 100:5288–5294. https://doi.org/10.1016/j.biortech.2009.05.019

Wassén S, Bordes R, Gebäck T et al (2014) Probe diffusion in phase-separated bicontinuous biopolymer gels. Soft Matter 10:8276–8287. https://doi.org/10.1039/c4sm01513d

Wu N, Hubbe MA, Rojas OJ, Park S (2009) Permeation of polyelectrolytes and other solutes into the pore spaces of water-swollen cellulose: a review. BioResources 4:1222–1262

Yang D, Moran-mirabal JM, Parlange J, Walker LP (2013) Investigation of the porous structure of cellulosic substrates through confocal laser scanning microscopy. Biotechnol Bioeng 110:2836–2845. https://doi.org/10.1002/bit.24958

Zhang Y, Cai L (2006) Effects of steam explosion on wood appearance and structure of sub-alpine fir. Wood Sci Technol 40:427–436. https://doi.org/10.1007/s00226-005-0053-6